A Computational Investigation of Closed Timelike Curves and Embedded Geometry in General Relativity

Yuvan Raam Chandra
Email: yuvanraam1805@gmail.com
Mailing Address: 10 Jln Rengas, Seletar Hills Estate,
Singapore 808530

March 31, 2026

Abstract

This paper presents a computational study of light-cone tipping, chronology-sensitive structure, and embedded spatial geometry in general relativity using a custom metric-driven workflow. The aim is to show how a user-specified metric can be analyzed directly through symbolic tensor computation, numerical geodesic integration, reduced-slice embedding, and diagnostic energy plotting. The framework is designed to adapt to different metrics in a unified way. Gödel spacetime is used as the principal example because it makes cone tipping and the chronology threshold especially transparent, while a Kerr-type sector is included to show that the same computational machinery can be transferred to a second metric class. The emphasis throughout is on visualization, reproducibility, and geometric interpretation.

Essay written for the Gravity Research Foundation 2026 Awards for Essays on Gravitation.

1 Introduction

General relativity describes gravity through spacetime geometry. Once a metric $g_{\mu\nu}$ is specified, it determines causal structure, geodesics, curvature, and the behavior of matter through the Einstein field equations. In many familiar spacetimes, the light cones preserve an ordinary local time ordering. In others, however, the cone structure can tilt strongly enough that chronology-sensitive behavior appears and, in some cases, closed timelike curves (CTCs) become possible.

The aim of this paper is computational rather than purely formal. Three connected tasks are emphasized:

(i) computing symbolic geometric quantities and selected Einstein-tensor components from a supplied metric,

(ii) integrating null and timelike geodesics numerically to visualize trajectories and cone structure,

(iii) constructing embedded diagrams of reduced spatial slices whenever the Euclidean embedding condition is satisfied.

The main contribution is a reusable code-based workflow. Instead of hard-coding one specific spacetime, the scripts are built to accept a user-defined metric and then generate the relevant geometric quantities and plots. This makes the project a computational investigation of how geometry, causality, and visualization interact across different spacetimes.

The pedagogical value is also central. The workflow exposes the chain of reasoning directly: one starts from the metric, computes the associated geometric quantities, identifies causal thresholds, and then visualizes the resulting null sheets, geodesics, or reduced slices. In that sense, the project is of interest to students because it gives a first-principles and reproducible route from the metric to chronology-sensitive structure in a very transparent way. More specialized numerical general relativity packages are often more sophisticated and more powerful, but they do not necessarily help students grasp as directly how the relativistic effect emerges from the metric itself.

2 Stationary Axisymmetric Setup

Many important examples involving frame dragging and chronology-sensitive behavior can be using a restricted stationary, axisymmetric ansatz. In the present work we take

$$ds^2 = -F(r)\,dt^2 + H(r)\,dr^2 + L(r)\,d\phi^2 + 2M(r)\,dt\,d\phi + H(r)\,dz^2, \tag{1}$$

where the metric functions depend only on r.

The coefficient $M(r)$ controls the off-diagonal $dt\,d\phi$ coupling and is responsible for rotational frame dragging. The coefficient $L(r) = g_{\phi\phi}$ is especially important for diagnosing chronology-sensitive regions. Because ϕ is periodic, the azimuthal curves

$$\gamma = \{t = \text{const},\ r = \text{const},\ z = \text{const}\}$$

are closed. Their invariant length is proportional to $L(r)$. If

$$L(r) < 0, \tag{2}$$

then these azimuthal circles become timelike and therefore define CTCs.

To understand light-cone tipping, consider null curves with $dr = dz = 0$. Imposing $ds^2 = 0$ in (1) gives

$$0 = -F(r)\,dt^2 + 2M(r)\,dt\,d\phi + L(r)\,d\phi^2. \tag{3}$$

Solving for the null slopes yields

$$\frac{d\phi}{dt} = \frac{-M(r) \pm \sqrt{M(r)^2 + F(r)L(r)}}{L(r)}, \tag{4}$$

or equivalently

$$\frac{dt}{d\phi} = \frac{-M(r) \mp \sqrt{M(r)^2 + F(r)L(r)}}{F(r)}. \tag{5}$$

These two branches determine the local future and past null directions in the (t, ϕ) plane.

As the metric coefficients vary with radius, the slopes vary as well, and the associated light cones tilt. When the tilt becomes strong enough that $L(r) < 0$, the azimuthal direction itself becomes timelike.

3 Reduced-Slice Embedding

A full four-dimensional spacetime cannot be plotted directly, so one studies reduced slices. For a constant-time, constant-polar-angle slice of a stationary axisymmetric metric, the induced two-dimensional metric takes the form

$$dl^2 = g_{rr}(r)\, dr^2 + g_{\phi\phi}(r)\, d\phi^2. \tag{6}$$

To embed this slice in Euclidean $\mathbb{R}^3$, use cylindrical coordinates (R, ϕ, z) with Euclidean line element

$$dl^2 = dR^2 + R^2\, d\phi^2 + dz^2. \tag{7}$$

Matching the angular coefficient gives

$$R^2 = g_{\phi\phi}(r). \tag{8}$$

Treating R as a function of r, one finds

$$dl^2 = \left[\left(\frac{dR}{dr}\right)^2 + \left(\frac{dz}{dr}\right)^2\right] dr^2 + R(r)^2\, d\phi^2. \tag{9}$$

Comparison with (6) gives

$$\frac{dz}{dr} = \pm\sqrt{g_{rr}(r) - \left(\frac{dR}{dr}\right)^2}, \tag{10}$$

which is valid only when

$$g_{rr}(r) \geq \left(\frac{dR}{dr}\right)^2. \tag{11}$$

These equations form the basis of the embedding code used here. The resulting surface is not the full spacetime, but the Euclidean embedding of a selected reduced slice. Even so, it gives a useful geometric picture of how that slice stretches or flares with radius.

4 Computational Workflow

The code is organized into three connected parts.

First, a symbolic script computes the inverse metric, Christoffel symbols, selected curvature quantities, and selected Einstein tensor components. Second, a numerical script integrates null and timelike geodesics. For axisymmetric examples, the visualization uses

$$x = r\cos\phi, \qquad y = r\sin\phi, \tag{12}$$

so the output appears in (x, y, t) coordinates. Third, an embedding script applies (8)–(11) to reduced spatial slices.

Taken together, these scripts provide a unified workflow: input a metric, compute the relevant geometric quantities, identify chronology-sensitive regions such as $g_{\phi\phi} < 0$, generate trajectory plots, and construct embedded diagrams of chosen slices. The scripts used to generate the figures are part of the pedagogical point of the project: the geometric steps are not hidden inside a black box, but can be followed directly from metric input to final plot. The code used to generate the figures in this paper is publicly available at: `https://github.com/Yuvan-a11y/General-Relativity-Timelike-Trajectory-Visualisation`

5 Gödel Spacetime

5.1 Metric and chronology threshold

Gödel spacetime provides a classic example of a rotating solution with chronology-sensitive behavior. Suppressing the spectator z-direction, the reduced metric can be written as

$$ds^2 = 2\omega^{-2}\left[-dt^2 + dr^2 - \left(\sinh^4 r - \sinh^2 r\right) d\phi^2 - 2\sqrt{2}\sinh^2 r\, dt\, d\phi\right]. \tag{13}$$

Comparing (13) with (1), one identifies

$$F(r) = 2\omega^{-2}, \qquad H(r) = 2\omega^{-2}, \qquad M(r) = -2\sqrt{2}\,\omega^{-2}\sinh^2 r, \qquad L(r) = 2\omega^{-2}\left(\sinh^2 r - \sinh^4 r\right). \tag{14}$$

The key coefficient is

$$g_{\phi\phi} = 2\omega^{-2}\left(\sinh^2 r - \sinh^4 r\right). \tag{15}$$

The azimuthal direction becomes null when $\sinh r = 1$, so the critical radius is

$$r_c = \operatorname{arcsinh}(1) = \ln\left(1 + \sqrt{2}\right). \tag{16}$$

For $r > r_c$, one has $g_{\phi\phi} < 0$, so the azimuthal circles are timelike.

5.2 Null hypersurfaces

Using (5), the null directions at fixed r are obtained from

$$0 = -dt^2 - 2\sqrt{2}\sinh^2 r\, dt\, d\phi + \left(\sinh^2 r - \sinh^4 r\right) d\phi^2.$$

Solving for $dt/d\phi$ gives

$$\frac{dt}{d\phi} = -\sqrt{2}\sinh^2 r \pm \sinh r \cosh r. \tag{17}$$

Integrating in ϕ at fixed r yields

$$T_\pm(r, \phi) = \left(-\sqrt{2}\sinh^2 r \pm \sinh r \cosh r\right)\phi + \text{constant}. \tag{18}$$

These surfaces show directly how the null directions tilt as r increases and how the cone structure changes near the chronology threshold.

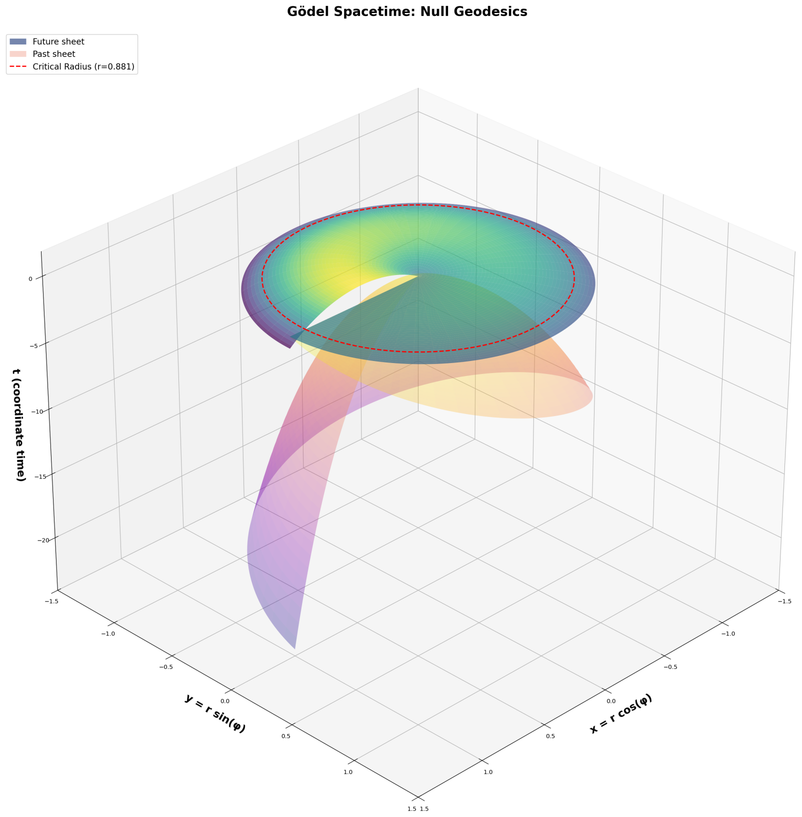

Figure 1: Null hypersurfaces in the reduced Gödel sector. The two sheets correspond to the future and past null branches determined by (18); the dashed circle marks the critical radius r_c.

5.3 Timelike geodesics and energy diagnostic

The trajectory code integrates timelike geodesics determined by the Christoffel symbols of the metric. These curves are useful for visualizing freely falling motion in the reduced (t, r, ϕ) sector. They do not by themselves constitute an explicit closed timelike curve construction; rather, they show how timelike trajectories respond to the geometry and how that motion sits relative to the chronology threshold.

The same reduced-sector treatment also allows a diagnostic scalar $\rho_{\text{eff}} = G_{\mu\nu}u^{\mu}u^{\nu}$ to be built from the Einstein tensor and a chosen stationary observer field on a stationary slice. In the Gödel case, this gives a visual diagnostic that complements the null hypersurface and geodesic plots.

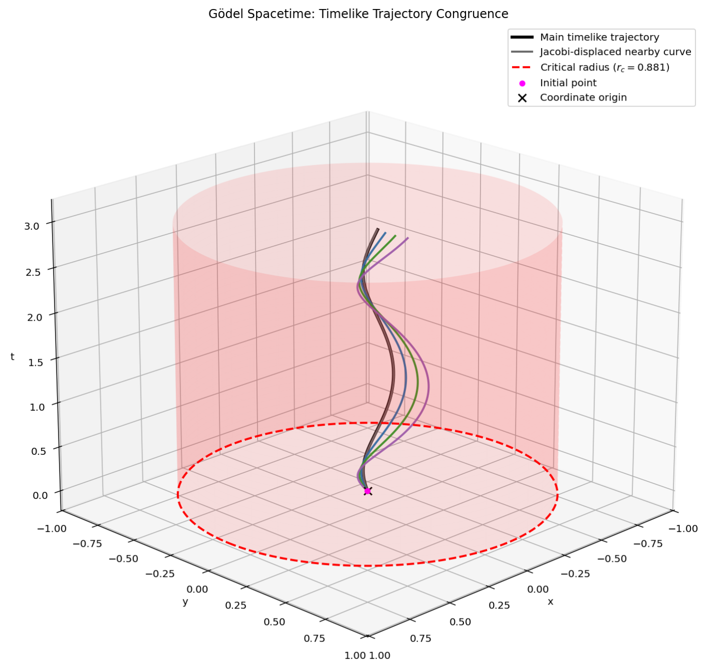

Figure 2: Timelike geodesic congruence in the reduced Gödel sector. The dashed circle marks the critical radius r_c, while the translucent cylinder indicates the corresponding chronology-sensitive region.

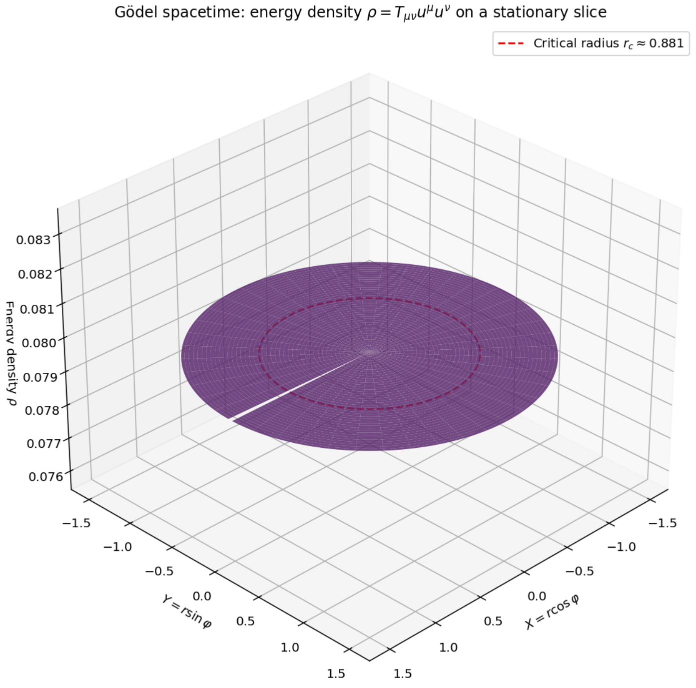

Figure 3: Energy-density diagnostic on a stationary Gödel slice, obtained from the metric through the Einstein tensor and a chosen observer field.

6 Kerr-Type Geometry as a Second Example

Kerr-type metrics provide a second stationary-axisymmetric example. In Boyer–Lindquist-type coordinates, the Kerr metric contains nontrivial $g_{t\phi}$ terms associated with frame dragging. This makes it suitable for the same reduced-slice and trajectory analysis as in the Gödel case. The purpose of including Kerr here is not to reproduce a full causal analysis of that spacetime, but to show that the code is not tied to one fixed example. The same computational pipeline can be adapted to Kerr-type geometries by changing the metric input and the slice selection.

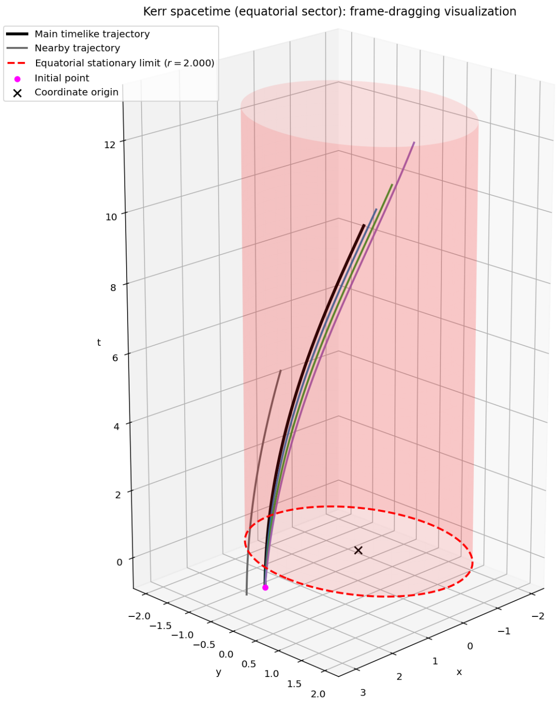

Figure 4: Representative Kerr-sector visualization included to show that the same computational workflow can be adapted to a second metric class. Here the emphasis is on frame dragging rather than on an explicit chronology construction.

7 Discussion and Conclusion

The main result of this investigation is a practical computational framework for studying unusual causal geometry directly from a user-specified metric. The framework combines symbolic tensor computation, numerical trajectory integration, embedded-slice visualization, and diagnostic curvature or energy plotting in a single workflow.

The Gödel example shows how the code captures cone tipping and the chronology threshold through the sign change of $g_{\phi\phi}$. The null hypersurface plot visualizes the two local null branches, the timelike geodesic plot shows representative motion in the reduced sector, and the energy diagnostic gives a complementary curvature-based view of the same geometry. The Kerr example shows that the same computational method can be adapted to a second metric class without redesigning the entire pipeline.

These reduced visualizations do not replace the full four-dimensional geometry. Instead, they make certain aspects of it easier to interpret. Constant-time slices, null sheets, embedded diagrams, and reduced trajectory plots provide a controlled way to display cone tipping, frame dragging, and chronology-sensitive thresholds in a form that can be checked directly against the metric.

By keeping the workflow first-principles, transparent, and reproducible, the project shows students directly how relativistic effects can be traced from the metric to the resulting reduced visualization. In this sense, the work serves both as a computational investigation and as a bridge between formal general relativity and visual understanding.

References

[1] K. Gödel, *An Example of a New Type of Cosmological Solutions of Einstein's Field Equations of Gravitation*, Rev. Mod. Phys. **21**, 447–450 (1949).

[2] S. W. Hawking, *The Chronology Protection Conjecture*, Phys. Rev. D **46**, 603–617 (1992).

[3] R. M. Wald, *General Relativity*, University of Chicago Press, Chicago (1984).

[4] F. S. N. Lobo, *Closed timelike curves and causality violation*, arXiv:1008.1127 [gr-qc].

[5] Y.-J. Han and H.-C. Lee, *Embedded Diagrams of Kerr and Non-Kerr Black Holes*, arXiv:1607.06535 [gr-qc].